Mission profile emulator for the power electronics systems of motor drive applications

Vernica, Ionut; Blaabjerg, Frede; Ma, Ke

Published in:
Proceedings of 2017 19th European Conference on Power Electronics and Applications (EPE'17 ECCE Europe)

DOI (link to publication from Publisher):
10.23919/EPE17ECCEEurope.2017.8099241

Publication date:
2017

Document Version
Accepted author manuscript, peer reviewed version

Mission Profile Emulator for the Power Electronics Systems of Motor Drive Applications

Ionuț Vernica, Frede Blaabjerg
Aalborg University
Pontoppidanstrde 111, 9220
Aalborg, Denmark
Email: iov@et.aau.dk, fbl@et.aau.dk

Ke Ma
Shanghai Jiao Tong University
800 Dong Chuan Rd, 200240
Shanghai, China
Email: kema@sjtu.edu.cn

Keywords

≪Adaptive control≫, ≪Drive≫, ≪Reliability≫, ≪Semiconductor device≫, ≪Variable speed drive≫.

Abstract

Due to the adverse temperature swings which normally occur in the power semiconductor devices during the start-up and deceleration periods of the motor drive system, the thermal design and control, as well as the reliability analysis of the power devices becomes crucial. In order to facilitate testing and access the loading and lifetime performances, a novel stress emulator for power semiconductor devices based on the mission profile of a motor drive system is proposed and designed. The control algorithm for the stress emulator setup is introduced, and the issues concerning the Orthogonal Signal Generator (OSG) are addressed by means of adaptive Notch filter implementation. Finally, experimental results are provided in order to validate the effectiveness of the proposed emulation technique.

Introduction

Nowadays, motor drive systems are being widely used in various mission-critical applications such as pump drives, fans, industrial production, mining, lift, etc., where the load changes frequently and fast. It is well known that the overall efficiency and reliability of the motor drive system is strongly dependent on the selected power semiconductor devices, and according to [1, 2], thermal cycling is one of the main causes of wear-out for the power devices. As a result, in order to predict the reliability performance and improve the design of the motor drive system, the thermal loading condition of the power devices needs to be more accurately assessed. However, the measurement/estimation of the thermal behaviour of the power semiconductor devices is still a challenging task, especially when considering real-field operating conditions or mission profiles of the motor drive system [3, 4].

Therefore, in order to solve the aforementioned problem, a novel mission profile emulation system is proposed in this paper. Based on a three-level Neutral Point Clamped (NPC) H-bridge converter, the dynamical voltage and current stresses of the power devices can be generated from the speed and torque profiles of the motor drive system. As a result, the actual loading profiles for the power semiconductor devices, considering the mission profiles of the converter, are reproduced. This approach will eliminate the need for an actual electric machine to be installed within the experimental setup and will allow for fast and accurate assessment of the thermal loading/reliability prediction of the power devices under various mission profiles and operating conditions.

First, a typical motor drive system is designed as a study case, and its dynamical behavior and frequency response are analyzed. Afterwards, an overview of the emulation technique, which targets to reproduce similar dynamics and loading behavior as for the given motor drive system is presented. Stability issues concerning the used Orthogonal Signal Generator (OSG) and the current controller employed for the

emulation strategy are emphasized, and a preliminary solution based on adaptive Notch filter implementation is proposed. Finally, the laboratory setup is described and the emulation technique is validated by means of experimental results.

Modeling and design of mission profile emulation technique

A typical motor drive application system is first selected as a study case. The system consists of a Permanent Magnet Synchronous Motor (PMSM) connected to the grid through a back-to-back three-level Neutral Point Clamped (NPC) converter, as shown in Fig. 1.

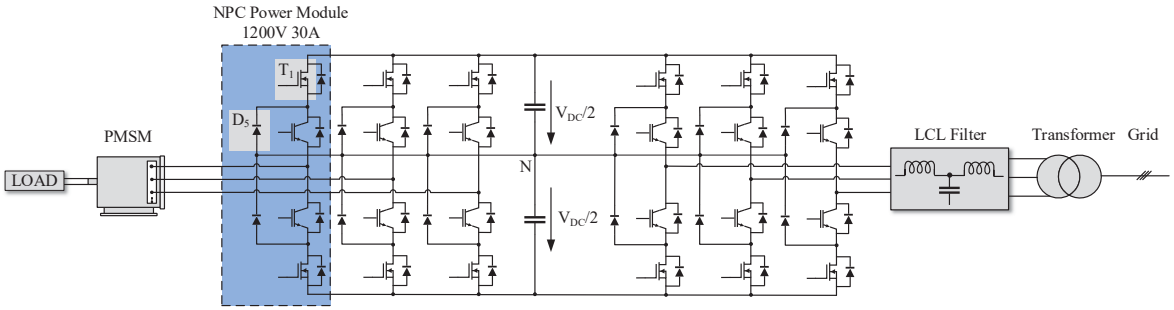

Fig. 1: Grid-connected motor drive system with back-to-back 3L-NPC.

The parameters of the machine are shown in Table I, while the power module choice is an IGBT module with a rated current of 30 A and a rated voltage of 1200 V.

Table I: Motor drive parameters.

Parameter	Symbol	Value	Unit
Output Power	P_n	9200	$[W]$
Nominal Voltage	V_n	350	$[V]$
Max. Current	I_{max}	21.43	$[A]$
Nominal Torque	T_n	12.55	$[Nm]$
Inertia	J	0.011	$[Kgm^2]$
Nominal Speed	n_n	7000	$[rpm]$
Number Pole Pairs	n_{pp}	1	[-]
Supply Voltage	V_{ll}	400	$[V]$
Switching Frequency	f_{sw}	16	$[kHz]$

The speed control of the motor is assured by means of Field Oriented Control (FOC), while the switching sequence of the power devices is generated by a Sinusoidal Pulse Width Modulation (SPWM) technique [5, 6]. The input torque and speed profiles of the motor drive system alongside with the torque and speed response of the PMSM are shown in Fig. 2, while the resulting three-phase currents and voltages of the motor under the given mission profiles are presented in Fig. 3.

From Fig. 3 it can be noticed that high current amplitude is generated by the motor during the acceleration period in order to meet the speed and torque requirements, while during the deceleration period the current will change its polarity and the power will flow from the machine towards the DC-link. The current amplitude and the fact that the machine operates at low fundamental frequency within certain periods, will lead to adverse thermal cycles which will result in a faster wear-out of the power devices [7]. Thus, it is of extreme importance that the proposed mission profile emulator setup is able to accurately reproduce the same dynamic voltage and current loading.

Based on the q-axis current control loop of the PMSM system [8], a Bode diagram of the open loop equivalent transfer function is shown in Fig. 4, where it can be noticed that the closed loop control for

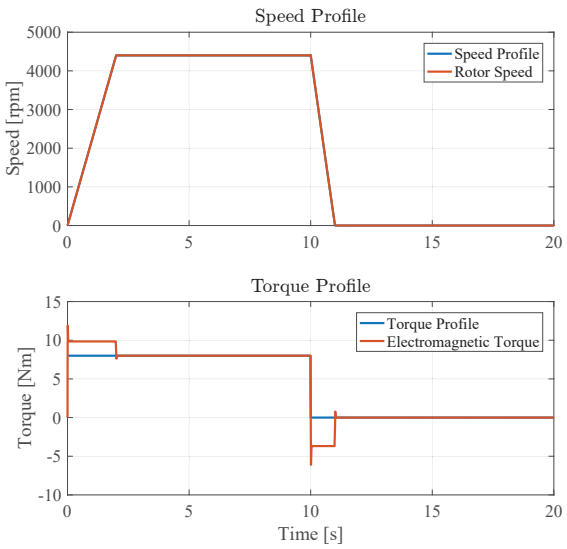

Fig. 2: Speed and torque mission profiles of the chosen motor drive study case.

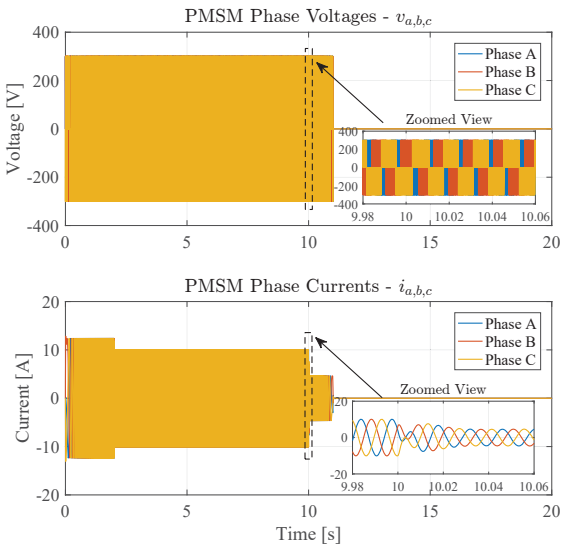

Fig. 3: Electrical response under given mission profiles and operating conditions.

for the q-axis current is stable with a bandwidth of 3830 rad/s. Similarly, from the time domain step response of the drive system, as shown in Fig. 5, it can be seen that the q-axis current has a rise time of 0.31 ms with an overshoot of 4.61%. This dynamic behaviour of the PMSM and control will be set as the design targets for the mission profile emulation system, which will then reproduce the same dynamic electrical/thermal stress on the power devices.

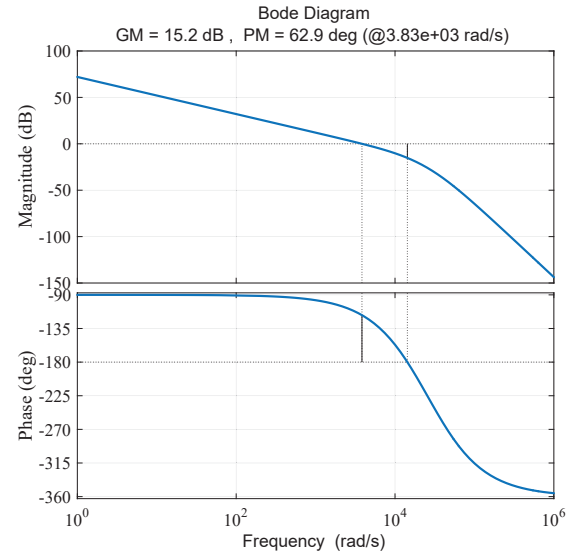

Fig. 4: Motor drive open loop Bode diagram.

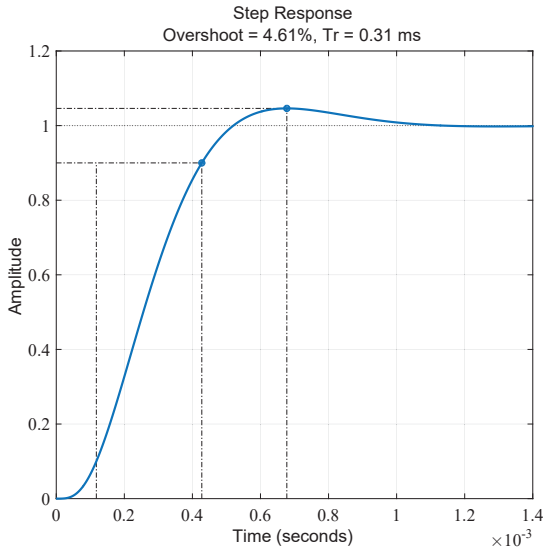

Fig. 5: Motor drive closed loop step response.

Configuration of emulation system

A general block diagram of the mission profile emulation system is shown in Fig. 6. By manipulating the *dq* reference frame equations of a PMSM [9], all the necessary parameters to assure the voltage and current control of the power devices can be obtained, taking into account the speed and torque profiles as inputs. Thus, based on the mechanical equation of the machine, the corresponding angle (θ) and electromagnetic torque (T_e) for the given mission profiles can be computed:

$$\theta = \int \omega_{ref} \cdot \frac{2\pi}{60} \tag{1}$$

$$T_e = \left(\frac{d\left(\frac{\omega_{ref} \cdot 2\pi}{60}\right)}{dt} \cdot J \right) + T_{load} \tag{2}$$

where, ω_{ref} represents the input speed mission profile, and T_{load} represents the torque mission profile.

By substituting the electromagnetic torque and electrical speed values into the torque and the voltage equations of the PMSM, the q-axis reference current (i_q^*) and the dq reference frame voltages can be determined.

$$i_q^* = \frac{2 \cdot T_e}{3 \cdot \psi_{pm} \cdot n_{pp}} \tag{3}$$

$$v_d^* = R_s i_d^* + L_d \frac{di_d^*}{dt} - \omega \psi_q \tag{4}$$

$$v_q^* = R_s i_q^* + L_q \frac{di_q^*}{dt} + \omega \psi_d \tag{5}$$

where, ψ_{pm} represents the permanent magnet flux linkage, R_s is the stator resistance, and L_s is the stator inductance.

Finally, the α component resulting from applying the inverse Clarke transformation to the reference d- and q-axis voltages (v_d^* and v_q^*) will represent the reference voltage for the test leg of the emulator setup (V_{test}). It should be noted that the reference d-axis current (i_d^*) is set to 0, in order to achieve the maximum torque per amp ratio. The resulting current reference values will represent the inputs to the current controller, which is used in order to generate the reference voltage for the load leg of the H-bridge inverter (V_{load}).

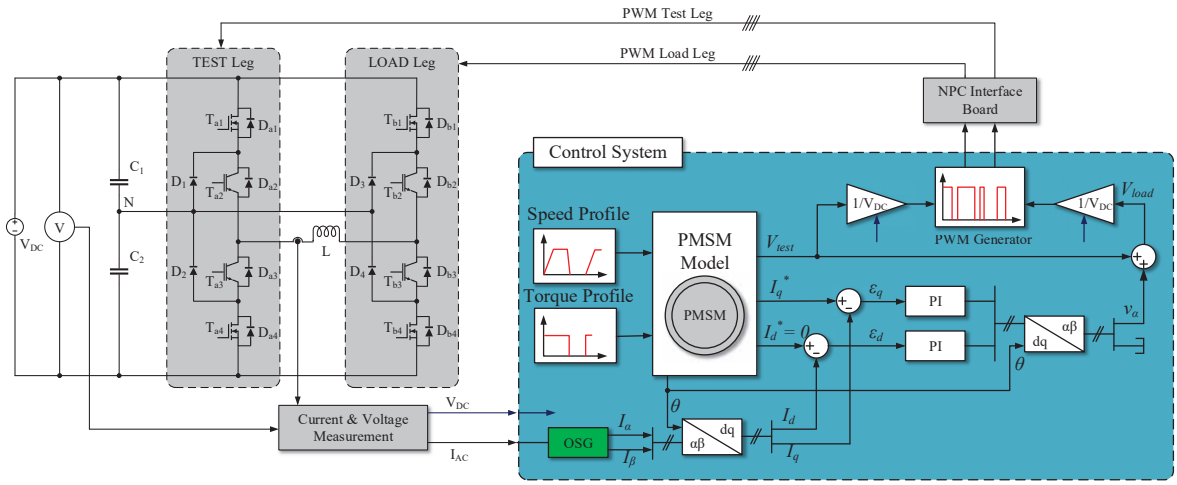

Fig. 6: Configuration of mission profile emulator setup.

As shown in Fig. 6 the stress emulator setup consists of a load leg and test leg. The legs of the three-level inverter are controlled independently, the PWM signals for each being determined by its corresponding reference voltage. The test leg is responsible for controlling the output AC voltage of the inverter, according to imposed modulation index and fundamental frequency requirements, while the load leg is used in order to control the output current [10].

Issues concerning Orthogonal Signal Generator (OSG)

Due to the fact that the employed converter topology in the emulation system consists of a single-phase H-bridge inverter, a 90^o phase shifted signal needs to be generated with respect to the output current, in order provide the necessary *dq* current values for the current controllers. Various methods for generating the quadrature component of an input signal have been studied throughout the literature [11]-[13], among which the Variable Transport Delay (T/4) and Second Order Generalized Integrator (SOGI) methods have shown the most promising results for the given application. The block diagrams of the two signal generating structures are shown in Fig. 7, respectively Fig. 8.

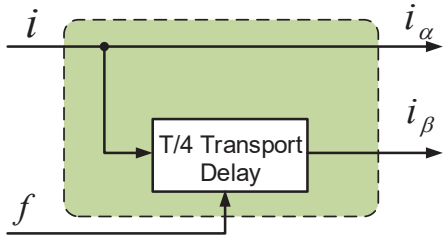

Fig. 7: Variable transport delay structure.

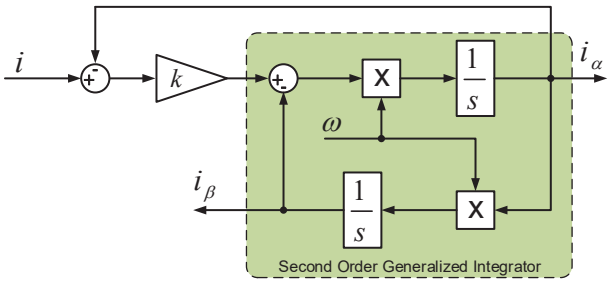

Fig. 8: SOGI structure.

The Laplace domain transfer function of the variable transport delay structure is shown in (6), where it can be noticed that this method is frequency dependent.

$$G_{T/4}(s) = e^{-s\cdot(f_s\cdot\frac{\omega}{8\pi})} \tag{6}$$

It is clear that although the T/4 method has a relatively simple implementation, through the use of a First-In First-Out (FIFO) buffer, including it into the system control loop, as shown in Fig. 11a will influence the overall dynamic behavior of the system. As it can be seen in Fig. 9, the T/4 method will result in a significant current overshoot during the acceleration period of the motor, while during the braking period a slow current response can be noticed. Thus, the current loading on the emulator inductive load, shown in Fig. 10, does not meet the mission profile emulator design requirements.

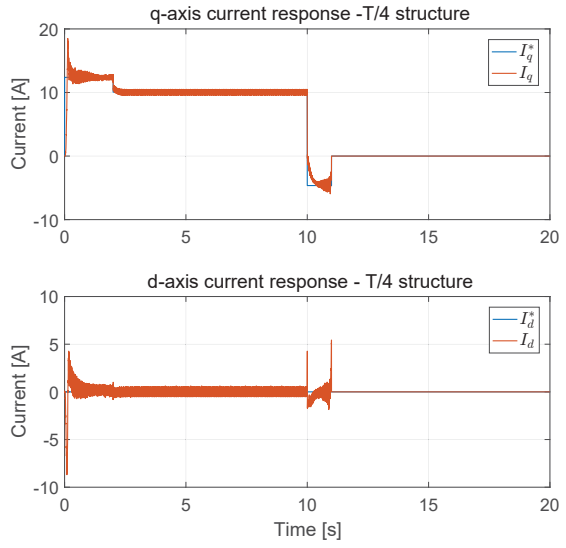

Fig. 9: d- and q-axis current for T/4 method.

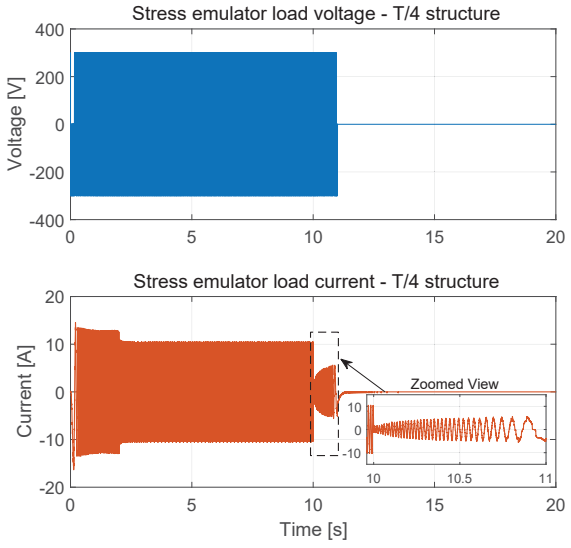

Fig. 10: Load current and voltage for T/4 method.

In the following the implementation of the SOGI method will be investigated. From Fig. 8 the closed-loop transfer functions of the structure can be determined:

$$H_d(s) = \frac{i_\alpha}{i}(s) = \frac{k\omega s}{s^2 + k\omega s + \omega^2} \tag{7}$$

$$H_q(s) = \frac{i_\beta}{i}(s) = \frac{k\omega^2}{s^2 + k\omega s + \omega^2} \tag{8}$$

where, k represents the gain of the SOGI structure.

Similarly to the previously presented OSG structure, the SOGI method is frequency dependent. Thus, when the machine operates outside the fundamental frequency (start-up and deceleration periods) the frequency response of the SOGI transfer function will vary as shown in Fig. 12.

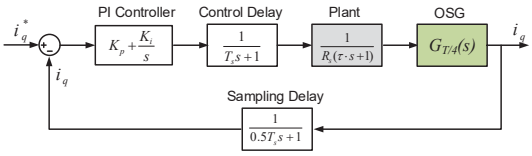

(a) Mission profile emulator with T/4 method.

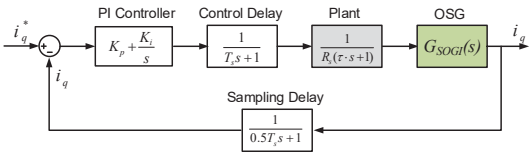

(b) Mission profile emulator with SOGI method.

Fig. 11: Emulator q-axis current control loop.

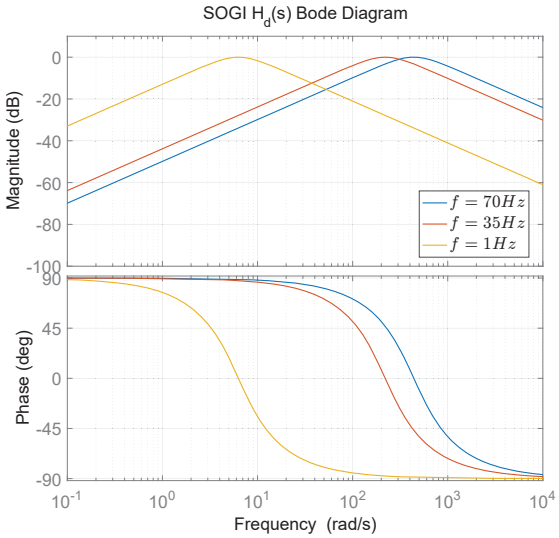

Fig. 12: Frequency response of SOGI.

By employing the SOGI method for generating the quadrature component of measured AC current of the emulator, and by inserting it into the current control loop, as shown in Fig. 11b, will lead to instability during the periods of time when the motor runs outside its designed fundamental frequency.

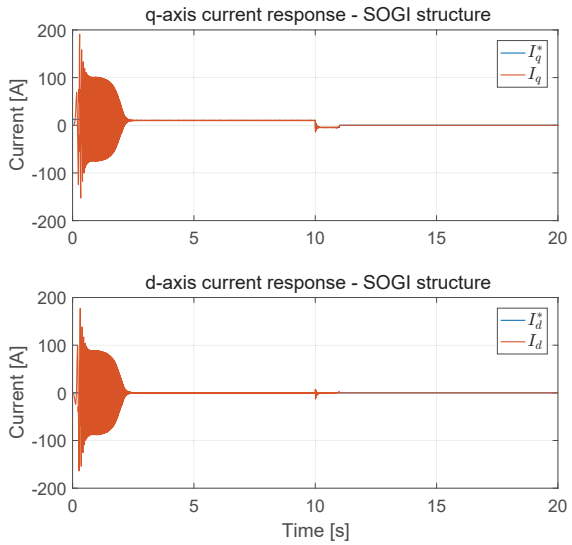

Fig. 13: d- and q-axis current for SOGI method.

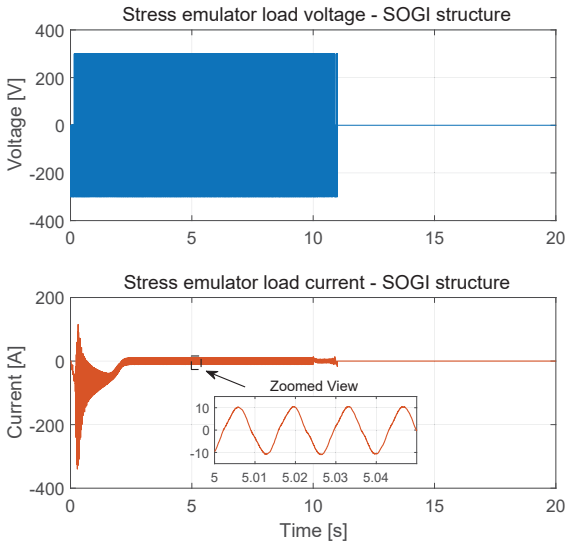

Fig. 14: Load stress for SOGI method.

The impact of the SOGI structure on the stability of the system can be seen in the d- and q-axis current response, shown in Fig. 13. From the voltage and current loading generated by the stress emulator plotted in Fig. 14, it is clear that during the 'constant speed' period, when the machine operates at nominal fundamental frequency, the system is stable and meets the design requirements.

Adaptive NOTCH filter implementation

A solution for the instability caused by the SOGI structure, based on implementing an adaptive Notch filter is described in the following. The Notch filter will generate an anti-resonance frequency of equal amplitude to the resonance frequency of the SOGI, and thus canceling-out its impact on the system and eliminating the frequency dependency of the current control loop.

The continuous transfer function used in order to design the Notch filter is presented in (9):

$$G_{Notch}(s) = \frac{s^2 + 2D_z\omega s + \omega^2}{s^2 + 2D_p\omega s + \omega^2} \tag{9}$$

All the parameters necessary for modeling the Notch filter have been analytically determined according to [14], and therefore, will allow for accurate tuning of the Notch filter for various fundamental frequency requirements. The frequency response of the Notch filter, together with the frequency response of the SOGI, can be seen in Fig. 16.

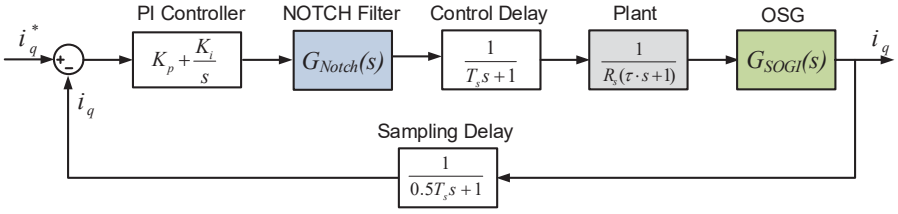

Fig. 15: q-axis current control loop with SOGI structure and Notch filter.

The Notch filter has been introduced within the system current control loop, as shown in Fig. 15, and its impact on the system stability has been analyzed. From Fig. 17 it can be seen that the voltage and current loading generated by the mission profile emulator meet the design requirements imposed by Fig. 3, and that the loading of the H-bridge inverter power module reproduces the actual stress of an power module used within a motor drive application with the given mission profiles and operating conditions.

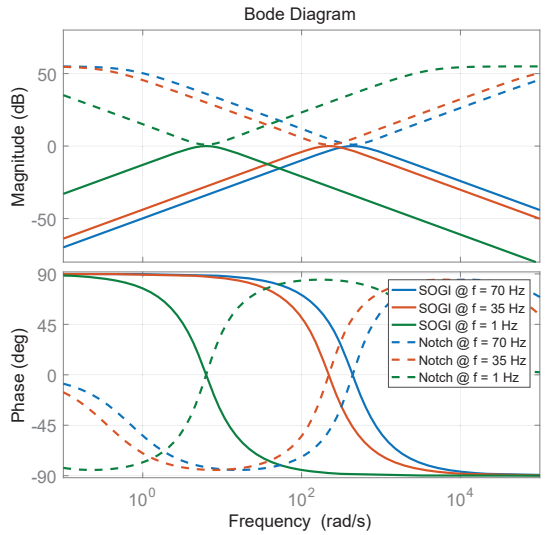

Fig. 16: Frequency response of SOGI and Notch filter for various frequencies.

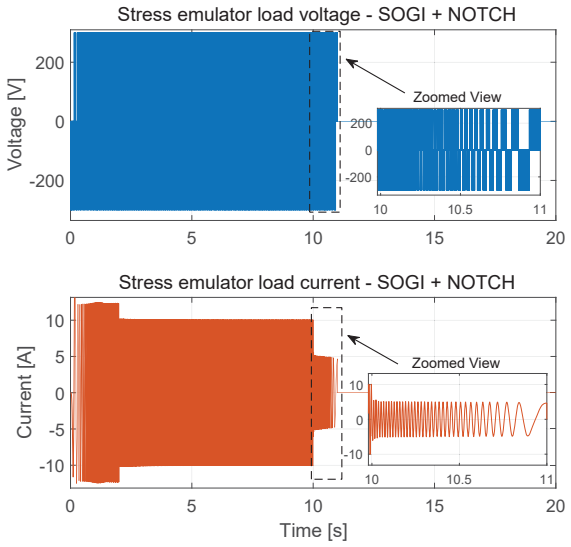

Fig. 17: Load current and voltage stress for SOGI method with Notch.

Although there are still some minor oscillations present within the current response of the stress emulator, this issue can be solved by optimizing the adaptive Notch filter design during the low fundamental frequency operation.

Experimental validation

In order to validate the emulation technique a dSpace-controlled 10 kW 3L-NPC H-bridge with an open IGBT module is employed. The setup allows for the emulation of different mission profiles of various real-life applications, among which motor drive systems. According the imposed speed and torque mission profiles, the motor drive load conditions will be emulated on the inductive load of the setup, and inherently on the power devices. This will allow for fast accurate measurement of the 'long-term' thermal behavior of the power devices, by means of thermal measurement equipment (e.g. infrared camera, optical thermal fibers, etc.). The mission profile emulator experimental setup is shown in Fig. 18.

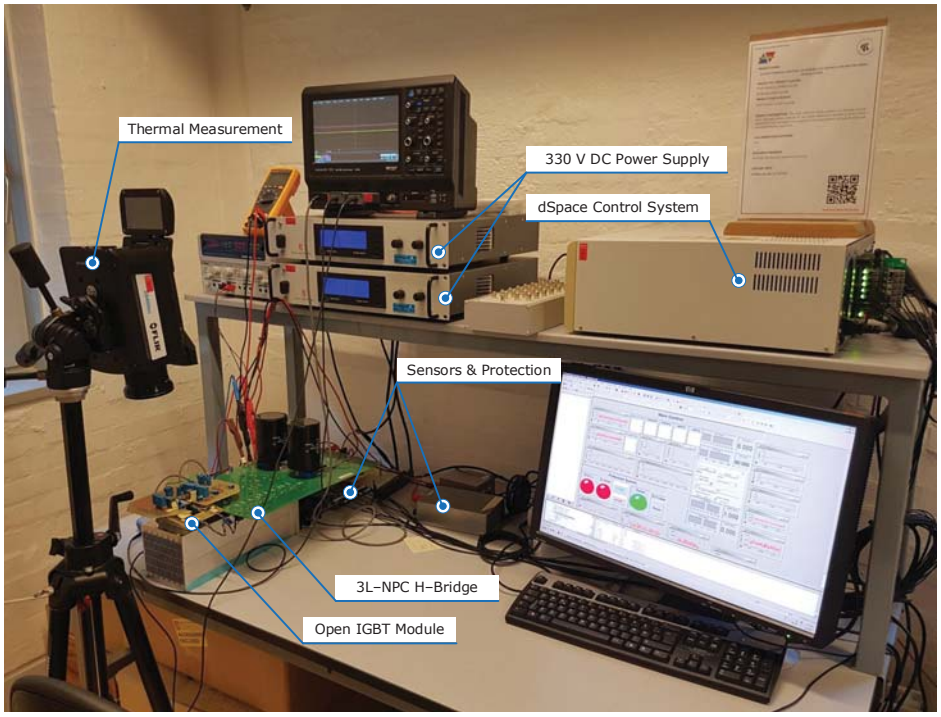

Fig. 18: Mission profile emulator experimental setup.

Initially, the Variable transport delay (T/4) method has been implemented, and as it can be seen from Fig. 19, the resulting current and voltage loading of the open IGBT module resembles the obtained simulation results. For the given OSG structure it can be concluded that it does not meet the design requirements for accurately emulating the current and voltage stress of the power devices.

The emulation technique, together with the SOGI structure and the Notch filter have been implemented with a dSpace Control Unit. It should be noted that the discrete implementation of both SOGI and Notch filter has been done by using the Trapezoidal method, where the integrator (1/s) has been approximated by:

$$\frac{T_s}{2}\frac{1+z^{-1}}{1-z^{-1}} \tag{10}$$

The experimental results for the proposed emulation technique, including the OSG-SOGI structure and the adaptive Notch filter are presented in Fig. 20. It can be seen that results match the design requirements, and that the mission profile emulator will generate similar current and voltage loading for the power devices as in an actual motor drive system. Additionally, this method will allow for accurate stress emulation independent of input speed and torque mission profiles, or machine parameters.

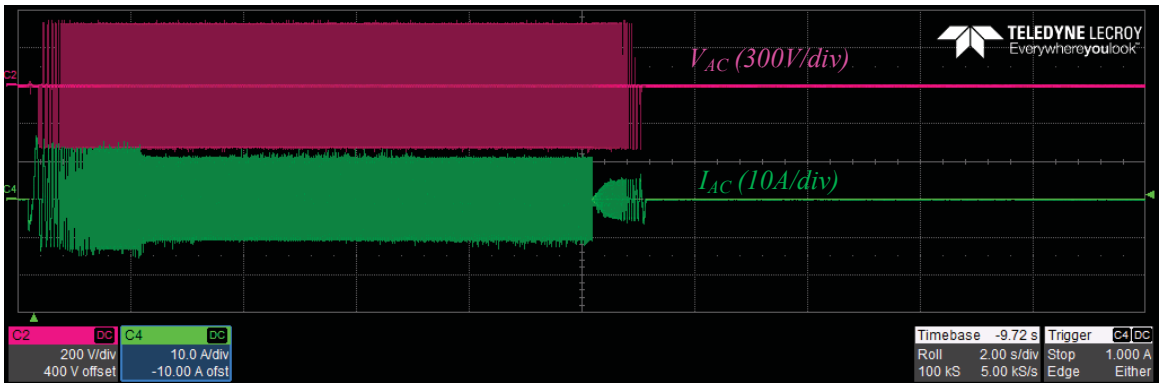

Fig. 19: Current and voltage loading on the open IGBT module for the T/4 method.

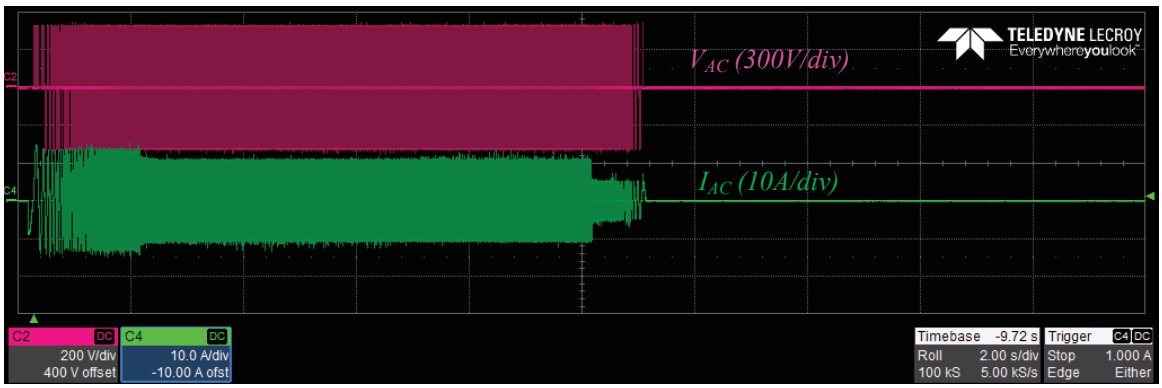

Fig. 20: Current and voltage loading on the open IGBT module for the SOGI+Notch filter method.

Conclusion

In this paper, a mission profile emulator setup for the power electronics of motor drive applications has been proposed. An initial motor drive system study case has been selected and its dynamic behavior has been investigated, and thus setting the design targets for the emulation technique. A detailed description of the emulator system and its control has been given, and the issues concerning the operation outside the fundamental frequency of two Orthogonal Signal Generating methods (Variable transport delay and SOGI) have been presented. A preliminary solution consisting of implementing an adaptive Notch filter has been proposed. It has been concluded that the proposed solution is able to accurately cancel-out the impact of the SOGI method on the stability of the system, and thus validating the emulation technique. Finally, experimental results have been presented, which validate the effectiveness of the mission profile emulator setup on reproducing similar voltage and current loading on the power devices, as in the motor drive study case, according to the given mission profiles and operating conditions.

References

[1] Ma K., Liserre M., Blaabjerg F., and Kerekes T.: Thermal loading and lifetime estimation for power devices considering mission profiles in wind power converter, IEEE Trans. on Power Electronics Vol. 30 no. 2, pp. 590-602

[2] Due J., Munk-Nielsen S., and Nielsen R.: Lifetime investigation of high power IGBT modules, EPE 2011-ECCE Europe, pp. 1-8

[3] Musallam M., Yin C., Bailey C., and Johnson M.: Mission profile based reliability design and real-life consuption estimation in power electronics, IEEE Trans. on Power Electronics Vol. 30 no. 5, pp. 2601-2613

[4] Bryant A. T., Mawby P. A., Palmer P. R., Santi E., and Hudgins J. L.: Exploration of power device reliability using compact device models and fast electro-thermal simulation, IEEE Trans. on Power Electronics Vol. 44 no. 3, pp. 894-903

[5] Lu K., Lei, X., and Blaabjerg F.: Artificial inductance concept to compensate nonlinear inductance effects in back EMF-based sensorless control method for PMSM, IEEE Trans. on Energy Conversion Vol. 28 no. 3, pp. 593-600
[6] Hava A. M., Kerkman R. J., and Lipo T. A.: Simple analytical and graphical methods for carrier-based PWM-VSI, IEEE Trans. on Power Electronics Vol. 14 no. 1, pp. 49-61
[7] Murdock D. A., Torres J. E. R., Connors J. J., and Lorenz R. D.: Active thermal control for power electronics modules, IEEE Trans. on Industry Applications Vol. 42 no. 2, pp. 552-558
[8] Phillips P. C, and Parr J. M.: Feedback control systems (5th Edition), Pearson, 2011
[9] Krause P. C., Wasynczuk O., and Sudhoff S. D.: Analysis of electric machinery and drive systems, John Wiley & Sons, 2002
[10] Choi U.-M., Jrgensen S., and Blaabjerg F.: Advanced accelerated power cycling test for reliability investigation of power device modules, IEE Trans. on Power Electronics Vol. 31 no. 12, pp. 8371-8366
[11] Mathe L., Iov F., Sera D., Torok L., and Teodorescu R.: Implementation of PLL and FLL trackers for signals with high harmonic content and low sampling frequency, OPTIM 2014, pp. 633-638
[12] Ciobotaru M., Teodorescu R., and Blaabjerg F.: A new single-phase PLL structure based on second order generalized integrator, Power Electronics Specialists Conference 2006, pp. 1-6
[13] Reza M. S., Ciobotaru M., and Agelidis V. G.: Robust technique for accurate estimation of single-phase grid voltage fundamental frequency and amplitude, IET Generation, Transmission & Distribution Vol. 9 no. 2, pp. 182-192
[14] Dannehl J., Liserre M., and Fuchs F. W.: Filter-based active damping of voltage source converter with LCL filter, IEEE Trans. on Industrial Electronics Vol. 58 no. 8, pp. 3623-3633